Electronic Supplementary Material (ESI) for RSC Advances.

Supporting Information

Stable cycling and Low-Temperature Operation Utilizing Amorphous Carbon-Coated Graphite Anodes for Lithium-ion Batteries

Pengfei Xiao[a], Zhongming Wang[a], Kecheng Long[a], Jixu Yang[a], Xinsheng Liu[a], Canhui Ling[a], Libao Chen[a,b], Lin Mei[a*]

[a] State Key Laboratory of Powder Metallurgy, Central South University, Changsha, 410083, P. R. China.

[b] National Energy Metal Resources and New Materials Key Laboratory, Central South University, Changsha, 410083, P. R. China.

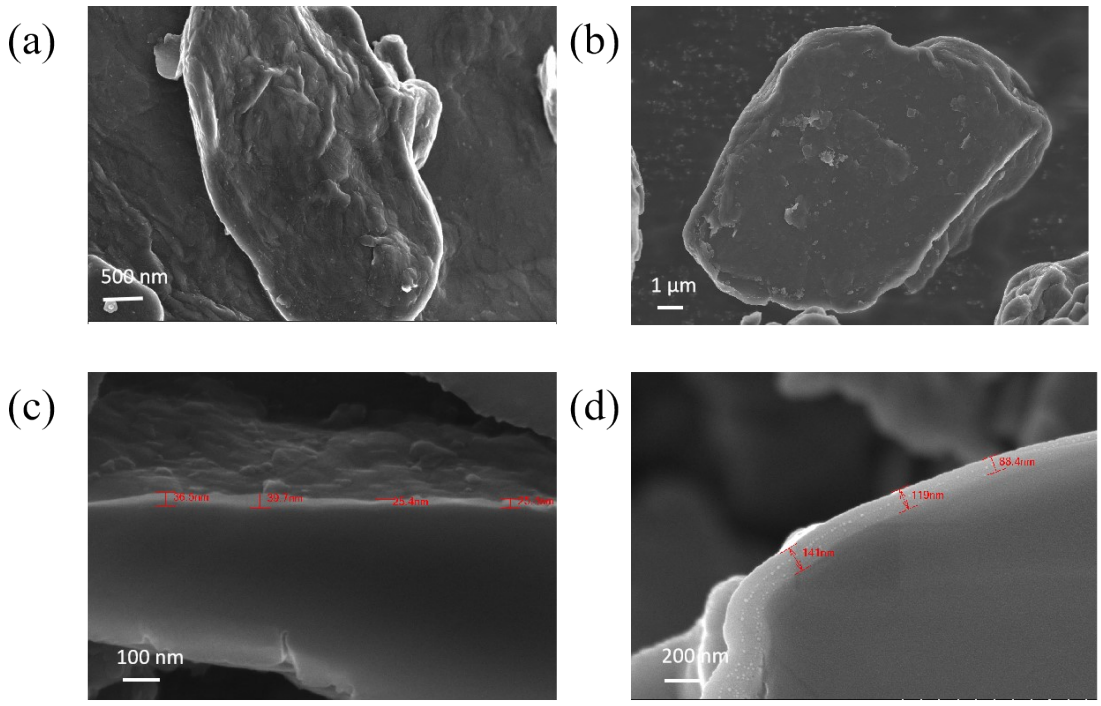

Figure S1. SEM images of GC-1 (a) and GC-3 (b); cross-section SEM of GC-1 (c) and GC-3 (d).

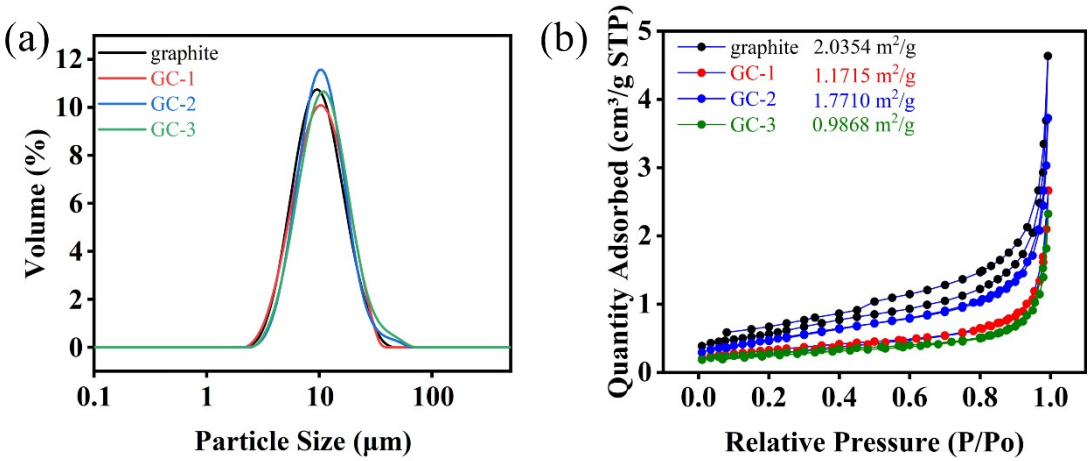

Figure S2. Particle size distribution chart (a); N2 adsorption and desorption isotherms (b).

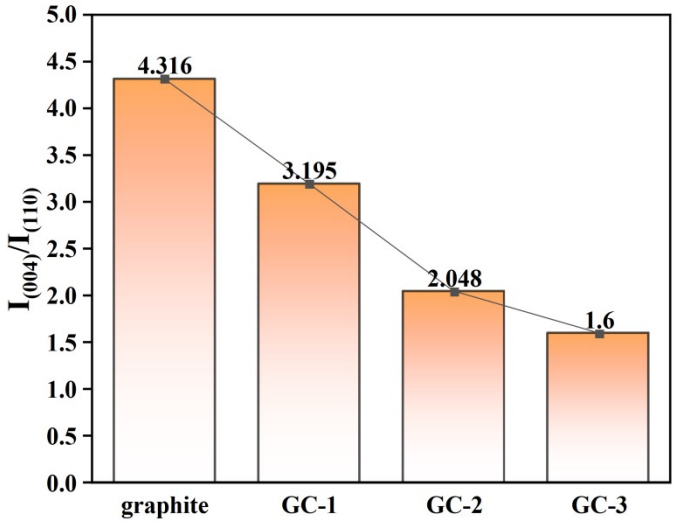

Figure S3. The OI value (the ratio of peak intensities of the (004) and (110) crystal faces) of samples.

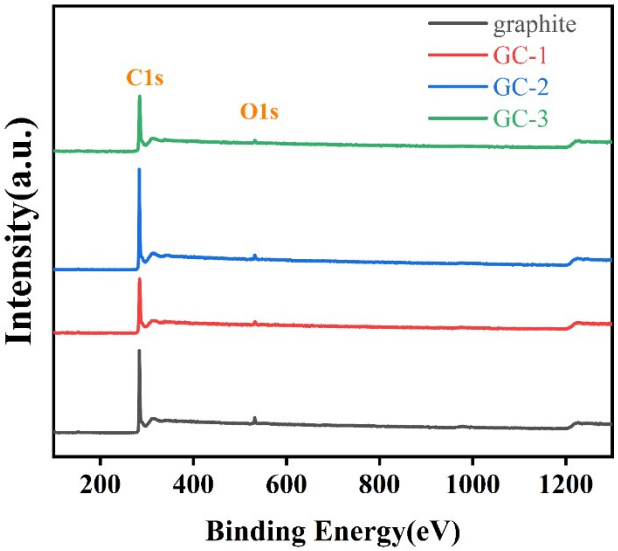

Figure S4. XPS analysis of graphite and GCs.

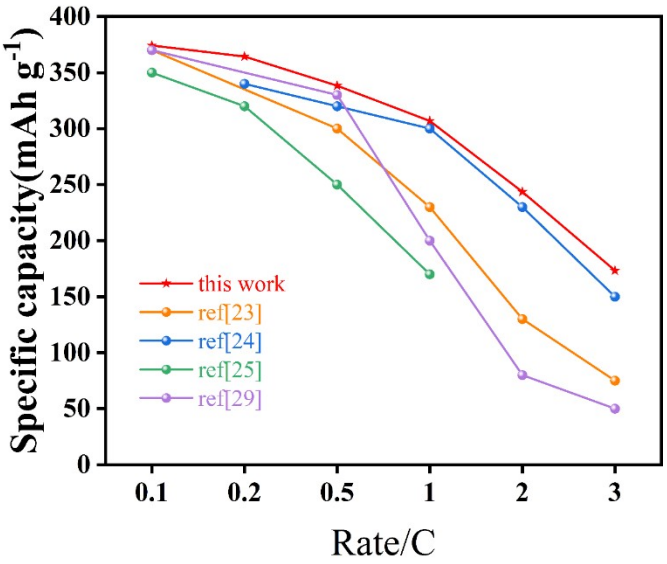

Figure S5. Rate performance of this work compared with relatived study.

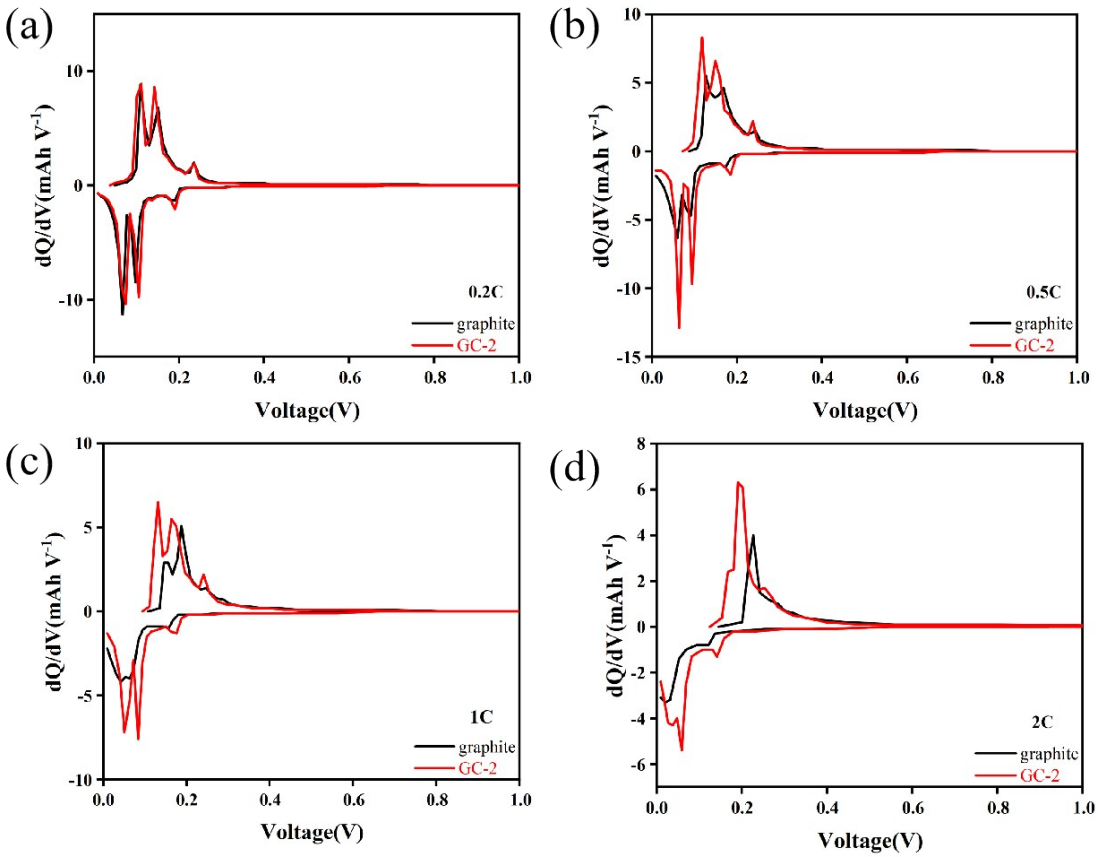

Figure S6. dQ/dV curves of pristine graphite and GC-2 at 0.2C (a), 0.5C (b), 1C (c) and 2C (d).

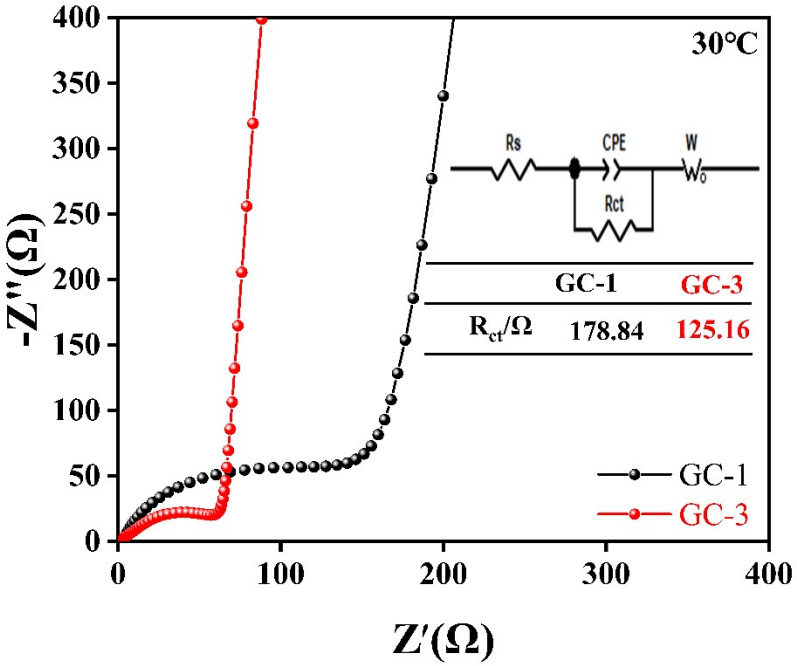

Figure S7. EIS Nyquist curves of GC-1 and GC-3 at 30 ℃.

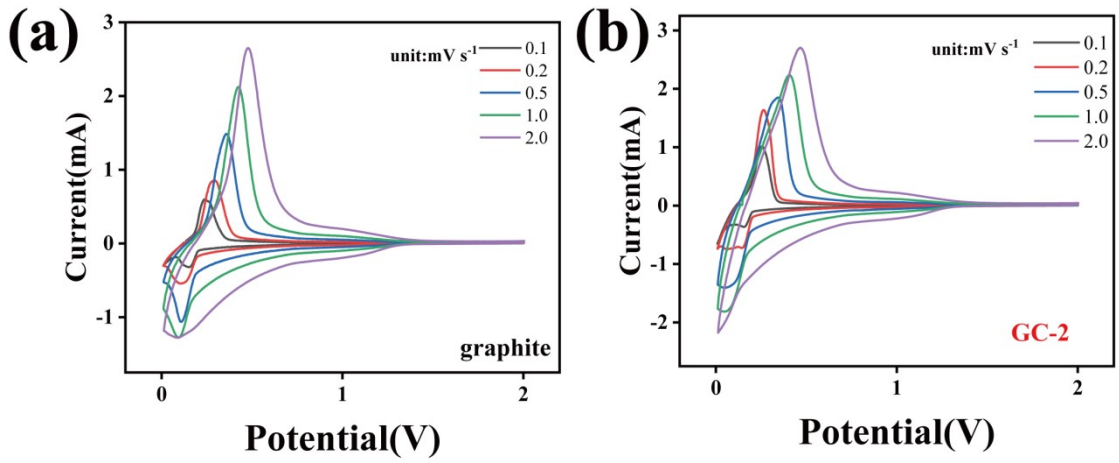

Figure S8. The CV curves at different sweep rates of pristine graphite (a) and GC-2 (b).

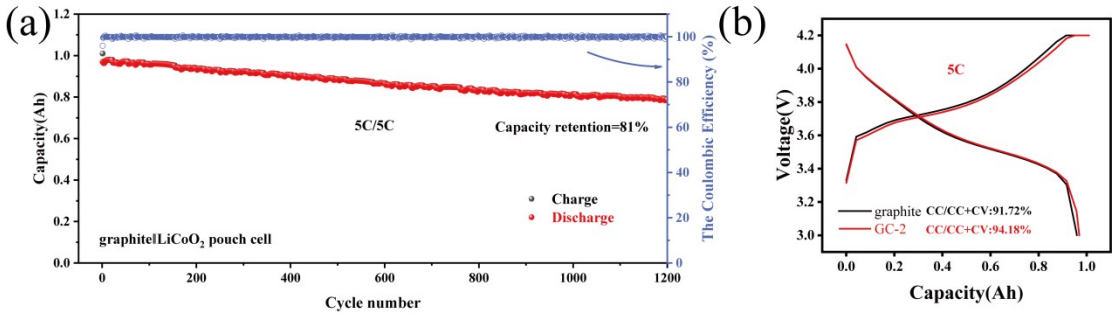

Figure S9. (a) graphite ‖ $LiCoO_2$ pouch cell cycles at 5C. (b) the charge/discharge curves of pouch cell at 5 C.

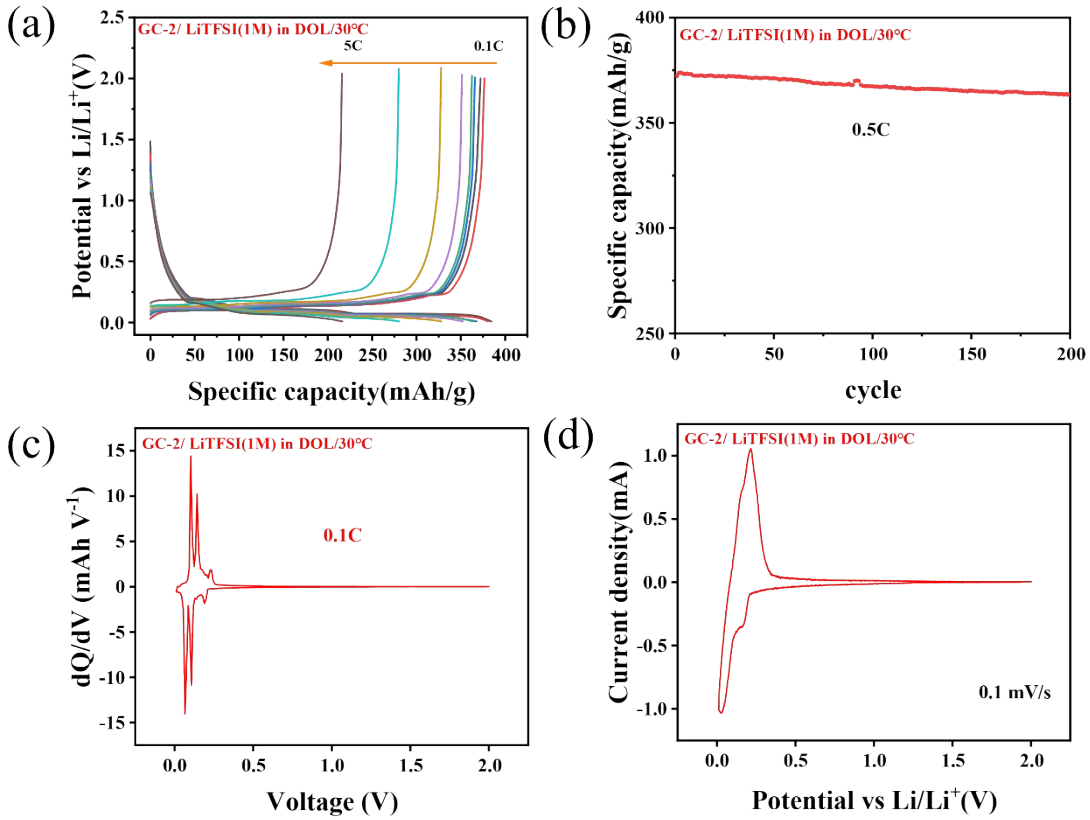

Figure S10. Electrochemical performance of GC-2 in DOL-based electrolytes at room temperature: (a) rate performance; (b) cycle performance at 0.5C; (c) dQ/dV curve at 0.1 C; (d) the CV curve at 0.1 mV s^{-1}.

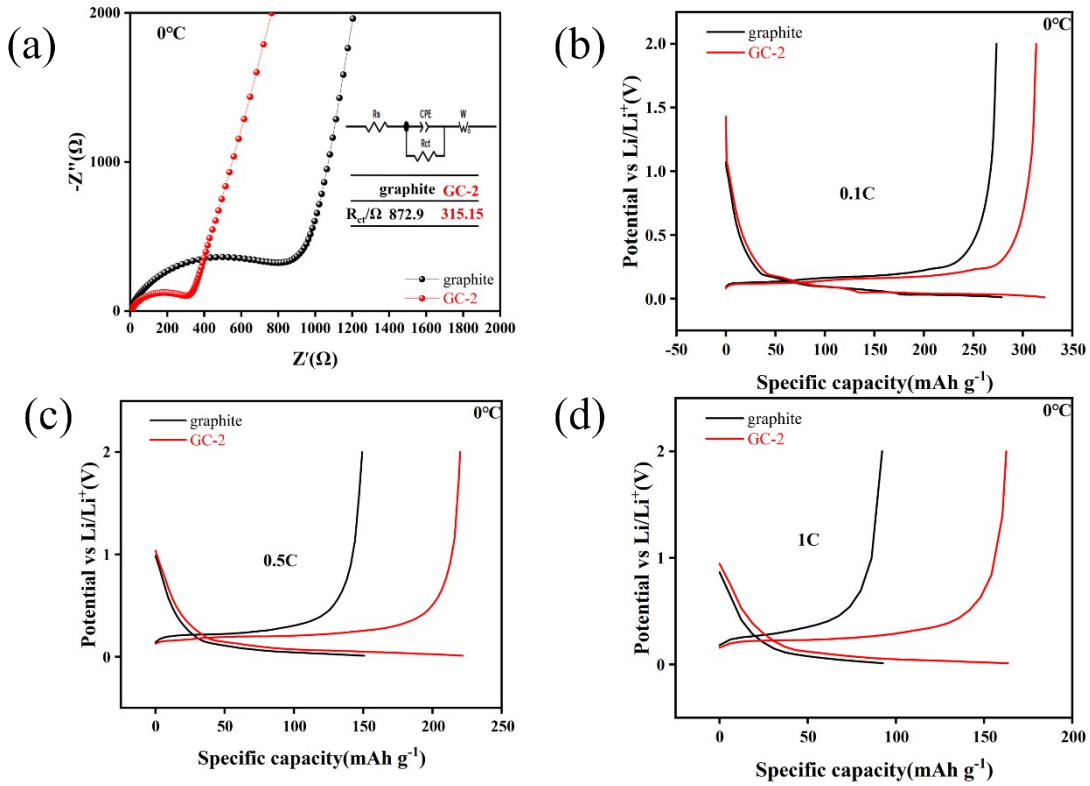

Figure S11. (a) EIS Nyquist curves at 0 ℃; (b-d) Charge/discharge curves at 0 ℃ from 0.1C to 1C.

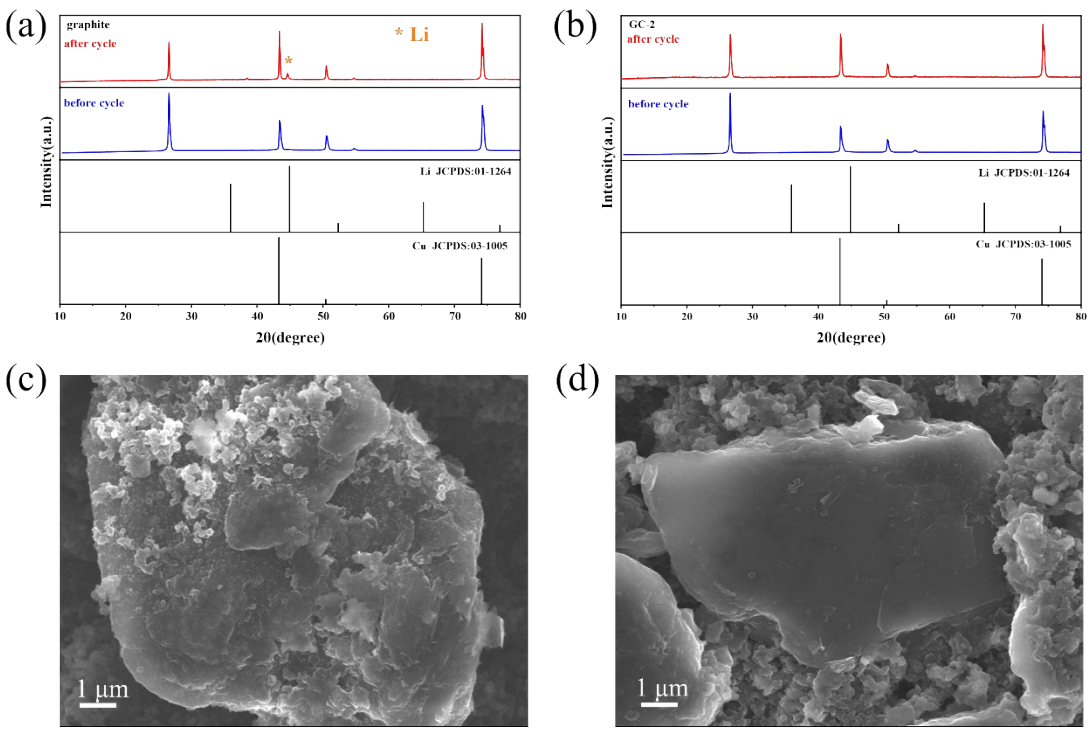

Figure S12. XRD patterns of electrode sheets before and after cycling at -20 ℃: graphite (a) and GC-2 (b); SEM images of graphite (c) and GC-2 (d) after cycling at -20 ℃.

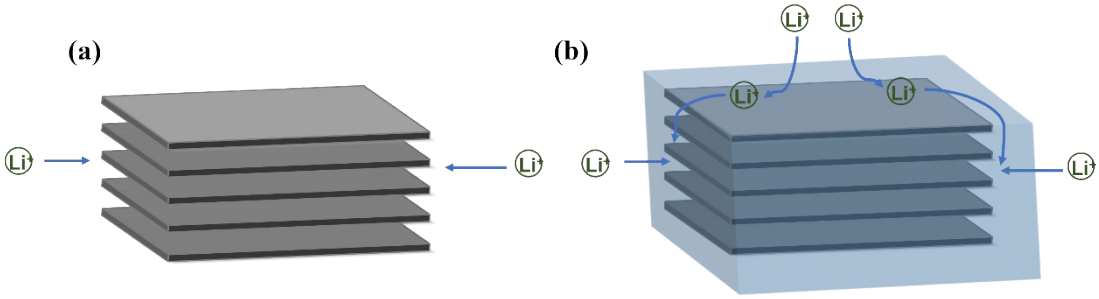

Figure S13. Mechanism diagram of amorphous carbon enhancement. (a) Lithium-ion can only enter the graphite from the end face, (b) Lithium-ion can pass through the amorphous carbon layer from the basal surface into the graphite.

Table S1. Rate performance of graphite and GCs.

Capacity/ (mAh g^{-1}) / Rate/C	graphite	GC-1	GC-2	GC-3
0.1	368.27	361.73	374.18	379.63
0.2	343.05	349.68	364.35	370.49
0.5	300.08	310.36	338.31	342.62
1	257.06	268.90	306.82	300.89
2	185.24	204.70	243.62	232.53
3	119.05	143.08	173.33	161.55
4	74.85	88.81	108.55	105.24
5	54.99	65.28	82.24	80.70